

## Multi-stimuli responsive shape memory polymers synthesized by using reaction-induced phase separation

Yufen Zhang,<sup>1</sup> Xue Jiang,<sup>1</sup> Ronglan Wu,<sup>1</sup> Wei Wang<sup>1,2</sup>

<sup>1</sup>Key Laboratory of Oil and Gas Fine Chemicals, Department of Chemistry, Xinjiang University, Urumqi 830046, China

<sup>2</sup>Department of Chemistry and Centre for Pharmacy, University of Bergen, Bergen N-5007, Norway

Correspondence to: W. Wang (E-mail: wei.wang@uib.no) and R. Wu (E-mail: wuronglan@163.com)

**ABSTRACT:** Thermo-induced multishape memory polymers are a growing focus of smart materials because of its promising applications. Multishape memory effect is generally attained by using polymers with broad phase transition and multiphase polymers. The latter is of particular interest for copolymerization and polymer compositing. One requirement has to be fulfilled to achieve multi-shape memory effect, which is to have two reversible phase transitions. In this study, we report synthesis of polymer composite composed of strong segregated polymers by using reaction-induced phase separation. We demonstrate the method by using polyurethane (PU) and poly(methacrylic acid) (PMAA). With adjusting the weight ratio, the polymer composites exhibit a phase spectrum from phase separation to miscible composite. The composite with PU/PMAA = 3:1 demonstrated triple-shape memory effect. Based on the results, we argued the effect of segregation on the shape memory effect for polymer composites. With the addition of PMAA, the polymer composite also exhibits pH/water-induced shape memory effect. © 2016 Wiley Periodicals, Inc. *J. Appl. Polym. Sci.* **2016**, *133*, 43534.

**KEYWORDS:** copolymers; functionalization of polymers; mechanical properties; polyurethane; stimuli-sensitive polymers

Received 12 October 2015; accepted 14 February 2016

DOI: 10.1002/app.43534

### INTRODUCTION

Shape memory polymers (SMPs) are smart materials that offer mechanical action triggered by external stimuli, such as heat, light, or moisture, etc.<sup>1–3</sup> This type of materials is able to remember one or more shapes, each determined by network elasticity.<sup>4</sup> Stress can be stored in a temporary shape by the immobilization of SMPs. This property can be realized by programming a sequence of polymer shapes that responds to respective stimulus.<sup>5,6</sup> As an example, a temporary shape can be programmed above the transition temperature of a dual-SMP. When the polymer is reheated above this temperature, the polymer may revert to its original shape. It has been argued that thermally induced dual-shape memory effect (SME) is an intrinsic property for all polymers because of the existence of thermal reversible phase transition at deformation temperature ( $T_d$ ), which may be either melting temperature ( $T_m$ ) or glass transition temperature ( $T_g$ ).<sup>7</sup> Recent research even exhibits that polymers with a broad temperature region of glass transition exert multi-SME (triple-SME and quadruple-SME), indicating the polymer can memorize more than two temporary shapes in a single shape memory cycle.<sup>8</sup>

SME is generally realized by reversible phase transition and freezing mechanism.<sup>9,10</sup> As a consequence, new multi-SMPs, in principle, can be synthesizing by blending two polymers with distinct reversible phase transitions. However, this underlying principle is difficult to be achieved in the synthesis of polymer composites. Early studies have shown that composites of two polymers with distinct  $T_d$ s may only exhibit dual-SME.<sup>11–13</sup> There is a fundamental dilemma in constructing a polymer composite with two distinct phase transition temperatures with regard to the compatibility of two components in the composite. Only one transition temperature exists in well-compatible composites; apart from that, phase separation occurs with incompatible components. In the later one, the mechanic properties of composites are greatly affected. This calls for the studies to discover the essential mechanism in synthesizing a macroscopically homogenous composite that satisfies the basic requirement of having two well-separated reversible phase transitions. Some enticing experiments were conducted to answer this question.<sup>14–18</sup> Xie *et al.* used macroscopic bilayer cross-linked polymers to achieve triple-SME.<sup>11</sup> The system could be considered as a macroscopically phase-separated system, while ingeniously connected by covalent bonds. This approach may easily be adopted in a bilayer construction, but can be

Additional Supporting Information may be found in the online version of this article.

© 2016 Wiley Periodicals, Inc.

difficult to fulfill for a polymer composition, especially with the strong interface. Macroscopically, polymer compositions with strong interface requires covalent bond to avoid phase separation, which is because of low mixing entropy.<sup>19</sup> Recent study has shown a different approach to this problem.<sup>20–22</sup> Chatani *et al.* used thiol-Michael addition reaction to connect two multifunctional thiol monomers with two multifunctional vinyls.<sup>21</sup> The study provided a method to construct a segregative polymer composite. Microscopically, the composite appeared as one polymer micro-particles embedded in another polymer matrix. This polymer composite exhibited excellent triple-SME with two distinct narrow glass transition regions.

Here, we conducted this study of synthesizing a polymer composite with a strong segregative system of polyurethane (PU) and poly(methacrylic acid) (PMAA) by using reaction-induced phase separation.<sup>23</sup> An immiscible polymer system can be understood by the reduction of mixing entropy when the degree of polymerization increases.<sup>24</sup> While, the monomers of a segregative system are commonly miscible before polymerization. This phase separation occurs during polymerization is called reaction-induced phase separation. Since the polymerization and phase separation occurs simultaneously, there is a competition between phase separation and the polymerization. This can lead to two extreme consequences, a total phase separation or a miscible composite. If the reaction rate is far above the diffusion of monomers, the competition will lead to a miscible composite, such as interpenetrating polymer network. Oppositely, if the diffusion of monomers is high in comparison to the reaction rate, the competition would result a total phase separation. Qualitatively, the competition can be determined by the sign of  $\chi - \{N/2[\Delta\phi(t)]^2\}$ .<sup>25,26</sup> Here,  $\phi$  is the volume fraction of one of the polymers,  $N$  the degree of polymerization, and  $\chi$  the interaction parameter between two components. When  $\chi > \{N/2[\Delta\phi(t)]^2\}$  is satisfied, the polymerization proceeds slower than the phase separation, and then the system tends to phase separate. While  $\chi < \{N/2[\Delta\phi(t)]^2\}$  is satisfied, the system becomes homogeneous because of the fast polymerization. This may suggest for a strong segregative system the reaction-induced phase separation is manageable by adjusting the volume ratio between two components when  $\chi$  and  $N$  are constant.

In the studied system, PU is a representative dual-SMP which consist of soft segments and hard segments. The soft segments form crystalline structure below  $T_d$  and melt above  $T_d$ ; hard segments often have high melting temperature, acting as physical net points.<sup>27</sup> The reason for choosing PMAA is that the  $T_d$  of PMAA is about 103 °C, which appears distinctly different from  $T_d$  of the soft segment of PU we utilized in our experiment.<sup>28</sup> The results suggest that with a chosen system with distinct phase transition temperature, it is possible to achieve multi-SME by changing the volume ratio of two components. Furthermore, PMAA contains carboxylic groups, creating high osmotic pressure after ionized in water. Thus, we may expect the composite to respond to multistimuli.

## MATERIALS AND METHODS

### Materials

Adipic acid (>99%), stannous chloride (SnCl<sub>2</sub>), and 1,4-butanediol (BDO, >98%) were purchased from Aladdin Industrial (Shanghai,

China). N,N'-dimethylformamide (DMF, >98%) and  $\alpha$ -methacrylic acid (MAA, >98%) were purchased from Kelong Chemical (Chengdu, China). N,N'-methylene bisacrylamide (BIS, >98%) was provided by Tianjin Chemical (Tianjin, China); 2,2'-azobis(1-methylpropionitrile) (AIBN) was purchased from Shanfu Chemical (Shanghai, China); 2,4-tolylene diisocyanate (TDI) was purchased from Damao Chemical (Tianjin, China); potassium persulfate (KPS, >99.5%) was purchased from Hengxing Chemical Crop. (Tianjin, China). DMF was dehydrated using 4Å molecular sieves, and then distilled before use. The rest reagents were used as received. Milli-Q water was used in all experiments with resistivity of 18 m $\Omega$ -cm.

### Synthesis of Poly(1,4-butylene adipate) Glycol (PBAG)

Adipic acid (120.01 g) and BDO (83.46 g) were added into a 500 mL four-necked flask with a graham reflux condenser, a thermometer, a Dean-Stark apparatus, and nitrogen flow. The mixture was first warmed up to 120 °C, then the temperature was kept between 120 °C and 160 °C for 12 hours in order to remove water in the mixture. The temperature raised to 200 °C afterwards to initiate the reaction. The reactants were kept at 200 °C for 2 hours, and then we vacuumed the flask in order to perform low-pressure isothermal color for 6 hours. The reaction yielded a flavescent viscous solution at high temperature, and the color became white after cooling to room temperature. PBAG as the soft segment of shape memory polyurethane (SMPU) is a polyol. The amount of hydroxyl group in terms of hydroxyl value was measured to be 23.02 mg NaOH/g and 0.54 mgHCl/g. As a result, the relative molecular weight of PBAG was calculated to be 3395 g/mol.

### Synthesis of PMAA Hydrogel

MAA (5.85 g) was mixed with 10 mL water in a vial, and further with 1 wt % KPS (0.23 g) and BIS (0.23 g). The mixed solution was reacted at 60 °C for 24 hours.

### Synthesis of PU

PBAG (4.05 g) and TDI (6.44 g) were mixed in a 100 mL flask. The mixture was stirred at 70 °C for 2 hours. The solution was cooled down to 60 °C, afterwards. BDO (3.15 g) was added into the mixture, and subsequently 20 mL DMF. The solution was stirred for another 2 hours, and cast into a thin film.

### Synthesis of PU/PMAA Composites

A stream of nitrogen flow was pumped into PU for 15 minutes before it was used. A mixture of MAA, BIS, and AIBN was added into PU solution. The amount of the materials is listed in Table I. Four PU/PMAA composites were realized with changing the weight ratio of PU and MAA. The reaction was performed at 60 °C for 2 hours. Then the mixture was cooled down to room temperature. The reaction yielded yellow viscous solution. The solution was transferred to a flat plate and cast into a thin film. The film was dried in a vacuum oven at 120 °C for 48 hours.

### Characterization of PMAA Gel, PU, and PU/PMAA

Fourier transform infrared spectra (FTIR) were measured for PMAA gel, PU, and PU/PMAA with IR Prestige-21 (Shimadzu, Japan). The PMAA gel was dried in vacuum oven at 60 °C for 12 hours before sample preparation. The sample was then

**Table I.** The Weight (gram) of Each Reactant for Synthesizing PU/PMAA Composites

PU:MAA (weight ratio)	PU	MAA	AIBN	BIS (2 wt %)	BIS (4 wt %)	BIS (6 wt %)
2:1	5.3374	2.6687	0.0525	0.0519	0.1018	0.1557
3:1	5.4237	1.8079	0.0361	0.0356	0.0709	0.1017
4:1	6.1904	1.5496	0.0345	0.0308	0.0617	0.0925
5:1	6.8872	1.3774	0.0296	0.0247	0.0523	0.0805

mixed with KBr and pressed into a disc. PU and PU/PMAA were measured directly. The wavenumber employed in the experiments was 400–4000  $\text{cm}^{-1}$ . Scanning electron microscopy (SEM) images were captured on LEO-143VP (LEO, Germany). We followed a standard protocol to prepare samples.<sup>29</sup> Samples were immersed in liquid nitrogen to obtain a brittle feature in order to prepare a fresh surface of cross section. The surface was then coated with gold particles. Differential scanning calorimetry (DSC) was carried out on DCS Q2000 (TA instruments, USA). Samples were treated with a protocol to eliminate any unknown thermal history before measurements. The heating and cooling procedures were repeated between 0 °C and 100 °C with a rate of 2 °C/min. Dynamic mechanical analysis (DMA) was measured on DMA Q800 (TA instruments, USA). A specimen was cut into cuboid with geometry parameters of 12 mm × 4 mm × 1 mm. The measurements were performed at 1 Hz, with a heating rate of 3 °C/min in a temperature range of 20–120 °C. Static tensile measurements were carried out on a benchtop tester H5KT (Tinius Olsen). The measurements were performed with an extension rate of 50 mm/min at room temperature. Contact angle measurements were carried out on a JJ2000B2 contact angle equipment (China) by using sessile drop method at room temperature. Contact angle was measured at five sites on each sample. We report the average value of the five measurements. The photographs for visual inspection are attached as Supporting Information.

### The Swelling of PU/PMAA

The swelling of PU/PMAA was evaluated by comparing the weight changes after the samples were immersed in water. All samples were first dehydrated in a vacuum oven for 12 hours at 120 °C. Swelling ratio ( $R_s$ ) was calculated by using the equation as follows.

$$R_s = \frac{W_a - W_b}{W_b} \times 100\% \quad (1)$$

In the equation,  $W_a$  and  $W_b$  represent the weight of samples after and before the swelling, respectively. The swelling experiments were performed of the specimens that contain different weight ratios and PU/PMAA. Water was used as a medium. The experiments were performed with five samples in parallel. We reported the average value of the five weights.

### Dual Shape Memory Effect

Shape memory properties were quantitatively evaluated by using a tensile and force controlled mode in thermal mechanical analysis set-up under ambient humidity condition.  $R_f$  and  $R_r$  for the

dual shape memory were calculated by using the equations as follows:

$$R_f(s_0 - s_1) = \frac{\epsilon_{s_1}}{\epsilon_{s_1,load}} \times 100\% \quad (2)$$

$$R_r(s_1 - s_0) = \frac{\epsilon_{s_1} - \epsilon_{s_0,rec}}{\epsilon_{s_1}} \times 100\% \quad (3)$$

where  $\epsilon_{s_1}$  represents the fixed strain after cooling and load removed,  $\epsilon_{s_1,load}$  represents the maximum strain under load,  $\epsilon_{s_0,rec}$  represents the strain after recovery, and  $(s_0 - s_1)$  and  $(s_1 - s_0)$  represent the change from original shape to shape 1 and the reverse, respectively. The demonstration of dual shape memory was carried out using oven heating. The sample strip was warmed up to 80 °C. After 5 minutes, the strip became soft and deformed to a helix. The shape was fixed at 0 °C. The helix was deformed again when warmed up to 80 °C.

### Triple Shape Memory Effect

We may expand eqs. (2) and (3) by adding eqs. (4) and (5) to quantitatively describe triple shape memory effect:

$$R_f(s_1 - s_2) = \frac{\epsilon_{s_2} - \epsilon_{s_1}}{\epsilon_{s_2,load} - \epsilon_{s_1}} \times 100\% \quad (4)$$

$$R_r(s_2 - s_1) = \frac{\epsilon_{s_2} - \epsilon_{s_1,rec}}{\epsilon_{s_2} - \epsilon_{s_1}} \times 100\% \quad (5)$$

For visual demonstration, the procedure is described as follows. A sample strip was warmed up to 80 °C. After the strip was softening, it was deformed to a primary helix. The helix was cooled down to 50 °C, and deformed to a secondary helix. This shape was fixed at 0 °C. The secondary helix was warmed up to 50 °C to recover to the primary helix, and then continued warming up to 80 °C to recover to the original shape. A video of triple-SME is available in Supporting Information.

### Water/pH-Induced Shape Memory

Water-induced shape memory effect was only performed with visual inspection. A sample strip was first warmed up to 80 °C. After softening, the sample was deformed and the shape was fixed by cooling it down to 0 °C in a water-ice bath. We put the sample in water at 25 °C to observe the recovery of the original shape. The same procedure was used for pH-induced shape memory.

## RESULTS

### FTIR Spectra of PBAG, PU, PMAA Gel, and PU/PMAA

The FTIR spectra of PBAG, prepolymer, and PU are presented in Figure 1(a). The characteristic absorption bands for PBAG appear at 2942  $\text{cm}^{-1}$  (asymmetric  $\text{CH}_2$  stretch), 1733  $\text{cm}^{-1}$  (free C=O stretch), 1263  $\text{cm}^{-1}$  (C-O-C asymmetric stretch),

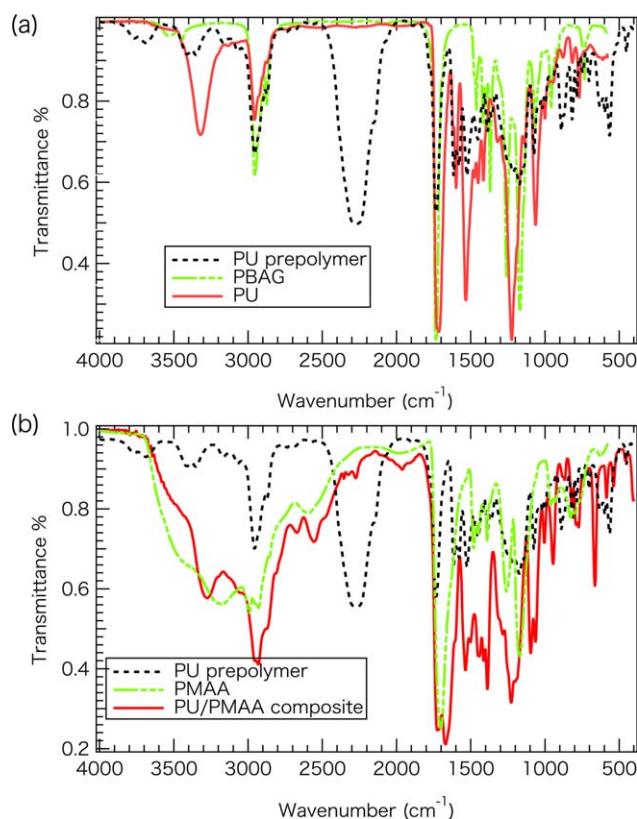


**Figure 1.** FTIR spectra of PBAG, PU, polyurethane prepolymer, and PU/PMAA. [Color figure can be viewed in the online issue, which is available at [wileyonlinelibrary.com](http://wileyonlinelibrary.com).]

and  $1175\text{ cm}^{-1}$  (C-O stretch). The absorption band for  $\text{N}=\text{C}=\text{O}$  is at  $2250\text{ cm}^{-1}$ , which can be observed in the spectrum of PU prepolymer. After the reaction, because of the depletion of  $\text{N}=\text{C}=\text{O}$ , we cannot observe the characteristic band at  $2250\text{ cm}^{-1}$  in the spectrum of PU. Instead, two characteristic bands exhibit at  $3322$  and  $1533\text{ cm}^{-1}$ , which are attributed to N-H stretching and bending vibrations. A similar result may be observed in Figure 1(b) for PMAA hydrogel, prepolymer, and PU/PMAA. The characteristic band for  $\text{N}=\text{C}=\text{O}$  absorption exhibits at  $2250\text{ cm}^{-1}$  for prepolymer, but not for PU/PMAA. N-H stretching and bending vibrations are also observed in the spectrum of PU/PMAA. This may indicate that the reactions of synthesizing PU and PU/PMAA were complete. Another observation in Figure 1(b) is that the C=O stretching shows two characteristic absorption bands at  $1730$  and  $1690\text{ cm}^{-1}$ . It is because of two types of C=O groups in PU/PMAA belonging to PU and PMAA, respectively, where in Figure 1(a) only the C=O stretching of PU is observed.

### Thermal Properties of PU And PU/PMAA

Thermal properties of PU and PU/PMAA were measured by DSC and DMA. Four specimens with different weight ratios of PU and PMAA were prepared as described in Material and Method section. Pure PU specimen was used as a reference. The DSC results of the specimens were presented in Figure 2. The pure PU shows an endotherm in the temperature range of  $30\text{--}60\text{ }^{\circ}\text{C}$ . This is ascribed to the melting of the crystalline soft phase, PBAG. This

endotherm may also be observed in the thermograph of the other specimens. For example, in the thermograph for PU/PMAA = 3:1, the melting temperature ( $T_m$ ) of the soft segment is at  $50.89\text{ }^{\circ}\text{C}$ , which is slightly higher than  $T_m$  for pure PU. In comparison with the pure PU, the PU/PMAA exhibits another endotherm in the DSC curves. This may be ascribed to the addition of PMAA, and the minimum of this endotherm changes with the weight ratio of PMAA. With increasing the ratio of PU/PMAA, this endotherm shifts towards lower temperature. It becomes less detectable for the specimen with the PU/PMAA ratio of 5:1. For the specimen with the PU/PMAA ratio of 3:1, this endotherm appears at  $84.43\text{ }^{\circ}\text{C}$ . The distinct two melting points may indicate phase separation in the PU/PMAA specimens. While, for the specimen with PU/PMAA = 2:1, the second endotherm has the minimum at nearly  $100\text{ }^{\circ}\text{C}$ , which is close to the  $T_g$  of pure PMAA.<sup>28</sup> This may indicate a total phase separation in the specimen.

Storage modulus is a measure of physical cross-linking density of segmented PU. The storage modulus ( $E'$ ) is presented as a function of temperature in Figure 3(a) for the samples with different weight ratios of PU/PMAA. All samples exhibit a decay in storage modulus with increasing temperature. For the sample with PU/PMAA at 3:1, the storage modulus reaches a short plateau at  $60^{\circ}$ , and the decrease of storage modulus becomes slow afterwards. These two decays are corresponding to the temperature range in the endotherm of the DSC curves. The storage modulus also increases to  $1900\text{ MPa}$ , which is much higher comparing to  $1500\text{ MPa}$  for PU. This may improve the shape memory effect because SMPs employing a higher storage modulus hold a faster recovery ratio.<sup>30</sup> For the other specimens, only one decay in the storage modulus is observed, and the storage modulus is of the similar value as for PU.

Figure 3(b) presents the plots of dissipation factor ( $\tan\delta$ ) vs temperature obtained from the DMA thermograms for all samples. The dissipation factor is associated with molecular mobility. The temperature-dependence of dissipation factor defines SME of polymers. All the samples exhibit a distinct dissipation peak in the temperature range of  $40\text{--}120\text{ }^{\circ}\text{C}$ . This temperature range is much higher than the melting temperature of soft

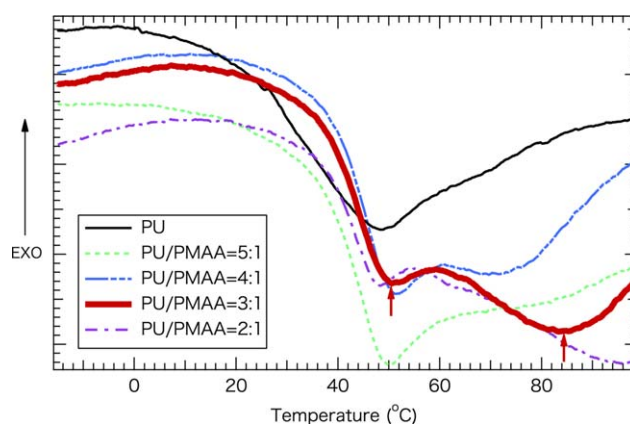


**Figure 2.** DSC curves of PU and PU/PMAA with different ratios of PBAG and MAA. The molar ratio of PBAG:TDI:BDO is 1:30:29. [Color figure can be viewed in the online issue, which is available at [wileyonlinelibrary.com](http://wileyonlinelibrary.com).]

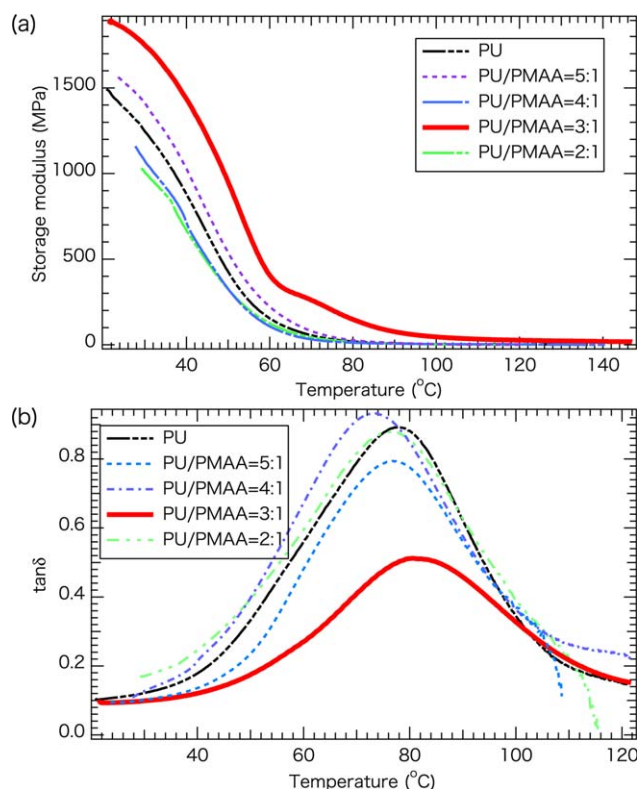


**Figure 3.** DMA curves of PU and PU/PMAA with different ratios of PBAG and MAA: (a) storage modulus, and (b)  $\tan(\delta)$ , defined as the ratio between loss modulus and storage modulus. [Color figure can be viewed in the online issue, which is available at [wileyonlinelibrary.com](http://wileyonlinelibrary.com).]

segments in PU. While this phenomenon is commonly observed, and ascribed to the melting of the soft segments superimposed on that of the hard phase in previous studies.<sup>27</sup> In Figure 3(b), we notice that the  $\tan\delta$  vs temperature for the specimen with PU/PMAA at 3:1 presents a different trend from others. The temperature range of transition is much wider than it for the other samples. The maximum of  $\tan\delta$  is about 0.5; while for other samples this value is between 0.7 and 1.

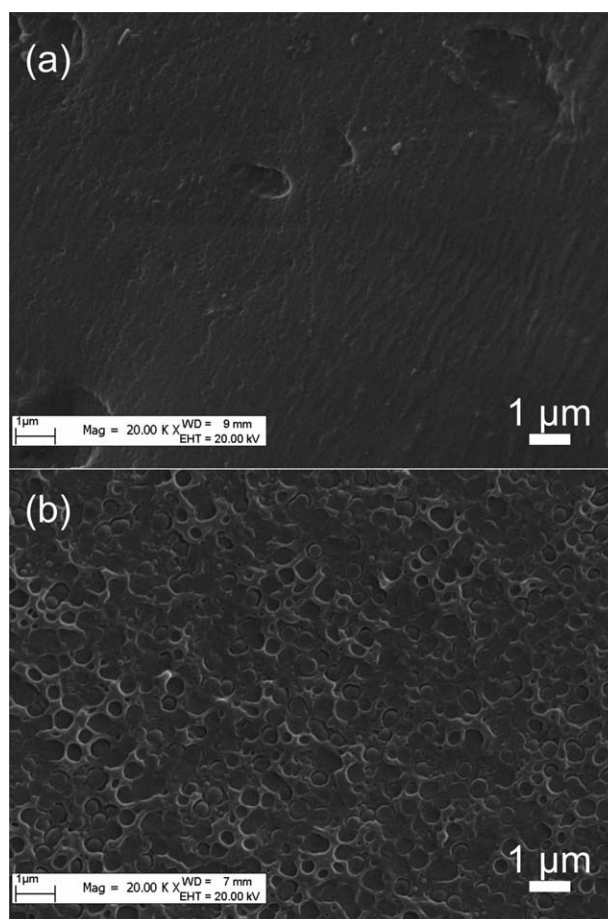
### SEM Results

Figure 4(a,b) show the morphology of the cross-sections of the fractured PU and PU/PMAA (3:1) specimens, respectively. The pure PU presents a homogenous and flat surface as shown in Figure 4(a). The addition of PMAA in the composite has completely changed the morphology on the fractured surface as shown in Figure 4(b). In comparing to the morphology in Figure 4(a), the fractured surface exhibits “sea island structure” for PU/PMAA (3:1). This structure is caused by the synthesis procedure. We performed an in-site polymerization in PU solution. This induced the phase separation in a micrometer scale, which we called reaction induced phase separation. The size of the pores on the surface is around 300–700 nm. Globular beads may be observed filling the pores, suggesting that the pores are not empty. Because of the poor compatibility of these two materials, there left a gap between the beads and the pores. The SEM images of the other specimens were also investigated (see Supporting Information), and no such structure was found for

the rest PU/PMAA composites. For PU/PMAA with the ratio of 4:1 and 5:1, the morphology of the composites are microscopically homogenous, which may indicate the composites form semi-interpenetrating polymer network. The morphology of the composite with the ratio of 2:1 exhibits phase separation in a large scale.

### Primary Shape by Dual SME

The thermally induced SME was investigated for all the specimens with different ratios of PU/PMAA. Only the specimen with PU/PMAA ratio of 3:1 exhibits good SME. Hence, it was chosen to demonstrate the dual SME and triple SME. We chose 80 °C to demonstrate the formation of primary shape by dual SME. Figure 5 presents the results of dual SME. The demonstration is presented by using a strip colored in blue. The shape of the strip was deformed at 80 °C, and forms a helix. It is cooled down to 0 °C to fix the temporary shape. The initial shape regained after the helix was warmed up to 80 °C. The recovery to its initial shape took only 5 seconds. The thermomechanical cycle can be quantified by programming the thermo cycle on DMA using controlled force mode. The stress–strain–temperature relation is presented on the bottom of Figure 5. The strain



**Figure 4.** SEM images of (a) PU and (b) PU/PMAA with  $W_{PU}/W_{MAA} = 3:1$ . The morphology of the polymer structure has changed after the addition of PMAA as comparing (a) and (b). Pure PU exhibits a smooth surface. While, as the presence of PMAA, the specimen exhibits a sea-island structure.

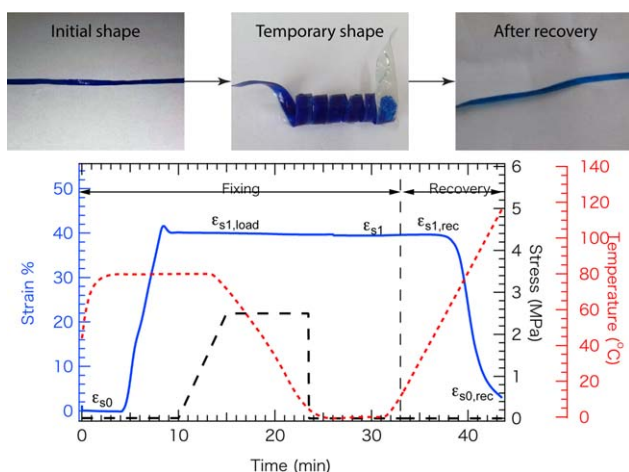


**Figure 5.** Visual demonstration of primary shape programmed by using dual SME (top). The strip warmed up to 80 °C, and formed helix shape (top middle). This shape was fixed at 0 °C, and can be recovered when the strip warm up again to 80 °C. The results of cyclic thermomechanical investigations for dual SME (bottom). The specimen was strain to 40% at 80 °C. Strain was unloaded, rendering  $R_f = 99\%$ ;  $R_r = 95\%$  after recovery. [Color figure can be viewed in the online issue, which is available at [wileyonlinelibrary.com](http://wileyonlinelibrary.com).]

fixity rate ( $R_f$ ) and the strain recovery rate ( $R_r$ ) are calculated to be 99% and 95%, indicating excellent shape fixity and recovery. The same experiment was repeated on the same sample three times. Both the strain fixity rate and recovery rate remained higher than 85%.

### Secondary Shape by Triple SME

A prototype triple SMP exhibits two shape fixations and recoveries. The triple SME requires a wide transition-temperature range. In the previous studies, this effect was often demonstrated by deforming the initial shape twice at two distinct positions. In the present study, we report a possibility to superimpose an imparted strain on the primary shape (such as the helix in dual SME), leading to a hierarchical SME. The superimposed shape is referred to as the secondary shape. This procedure is presented in Figure 6 (top). At the first step, a strip was shaped to a helix at 80 °C. The shape was fixed at 50 °C. Another helix deformation was superimposed on the primary helix, and this secondary shape was fixed at 0 °C. This programmed temperature cycle was used to measure the thermomechanical properties of the sample, and the result is presented in Figure 6 (bottom). The first temperature step at 50 °C leads to  $R_f(s_0 - s_1) = 94\%$ , which is lower than the value of  $R_f$  in the dual SME because the fixing temperature (50 °C) is within the transition temperature range. It suggests that the imparted strain has been partially recovered, which was observed in many systems of multi-SME with a wide temperature range.<sup>8</sup> However, with systems consisting two distinct transition temperatures, in the second shape transition,  $R_f(s_1 - s_2)$  was 97%. Subsequently,  $R_r(s_1 - s_0)$  and  $R_r(s_2 - s_1)$  were calculated to be 96% and 98%, respectively. The same thermomechanical cycle was performed on the same sample three times. Both  $R_r$  and  $R_f$  remained higher than 85%.

### Mechanical Properties of PU/PMAA

The SMP applications demand high mechanical properties. The respond of strain with applied stress was investigated on the specimen with PU/PMAA ratio of 3:1 with different cross-linker concentrations. The stress-strain curves are presented in Figure 7. The maximum strains corresponding to the ultimate stresses are presented in Table II. The results clearly show the increases of the maximum tensile strength and the maximum elongation with the content of cross-linker. The maximum tensile strength changed from 40 MPa (0 wt % BIS) to 62 MPa (6 wt % BIS), and the maximum strain increased from 259% (0 wt % BIS) to 375% (6 wt % BIS).

### Water/pH-Induced SME

The PU/PMAA specimens also responds to water and pH change in surroundings. These properties are highly correlated to the content of PMAA in the composites. With increasing the weight ratio of PMAA in the composite, the wettability of the specimen also changes. This can be monitored by contact angle (Supporting Information Figure 1). For the specimen with PU/PMAA ratio of 3:1, the contact angle with water was 38°. This result suggests that the surface of the material is hydrophilic, which is because of the considerable amount of PMAA. In spite of the change in hydrophobicity, the material contains carboxylic groups. The ionization of carboxylic groups will change with regard to the pH value of surroundings. Thus, pH-induced SME is expected. The images of the specimen after immersing in acidic, alkaline solutions, and water are presented in Figure 8(a). A coin-shaped specimen remains unchanged in water and HCl solution, but curls in NaOH solution. Figure 8(b) exhibits the water-induced SME. A curled specimen at dry state was immersed in water. The changes of polymer shape were recorded at different time points. After 20 minutes, the specimen has extended to a flat shape. Water/pH-induced SME is highly related to the diffusion of water inside the specimen. As the results of contact angle show, the hydrophilicity increases with the content of PMAA in the composite, which indicates that the specimen with PU/PMAA ratio of 2:1 may have the highest respond to water and pH change. This can be confirmed by swelling experiments. The swelling results of PU/PMAA of different weight ratios in water are presented in Figure 9. It shows that the PU/PMAA with ratio of 2:1 has the highest swelling degree. The swelling of PU/PMAA with the ratios of 4:1 and 5:1 are identical to the swelling of PU.

## DISCUSSION

### Temperature-Induced Triple SME

In the result section, we have demonstrated that the strong segregative system of PU/PMAA exerted triple-SME induced by thermal stimuli and water/pH responsive SME. The triple-SME attained by using polymer composites requires two reversible phase transitions, which is a general challenge in constructing polymer composites. With well-compatible polymers, the polymer composites often exhibit only one reversible phase transition; however, strong segregative system has need of covalent bond to form a composite with good homogeneity. In the introduction, two methods were presented in order to resolve this dilemma, covalent-bonded macroscopic bilayer and thiol-

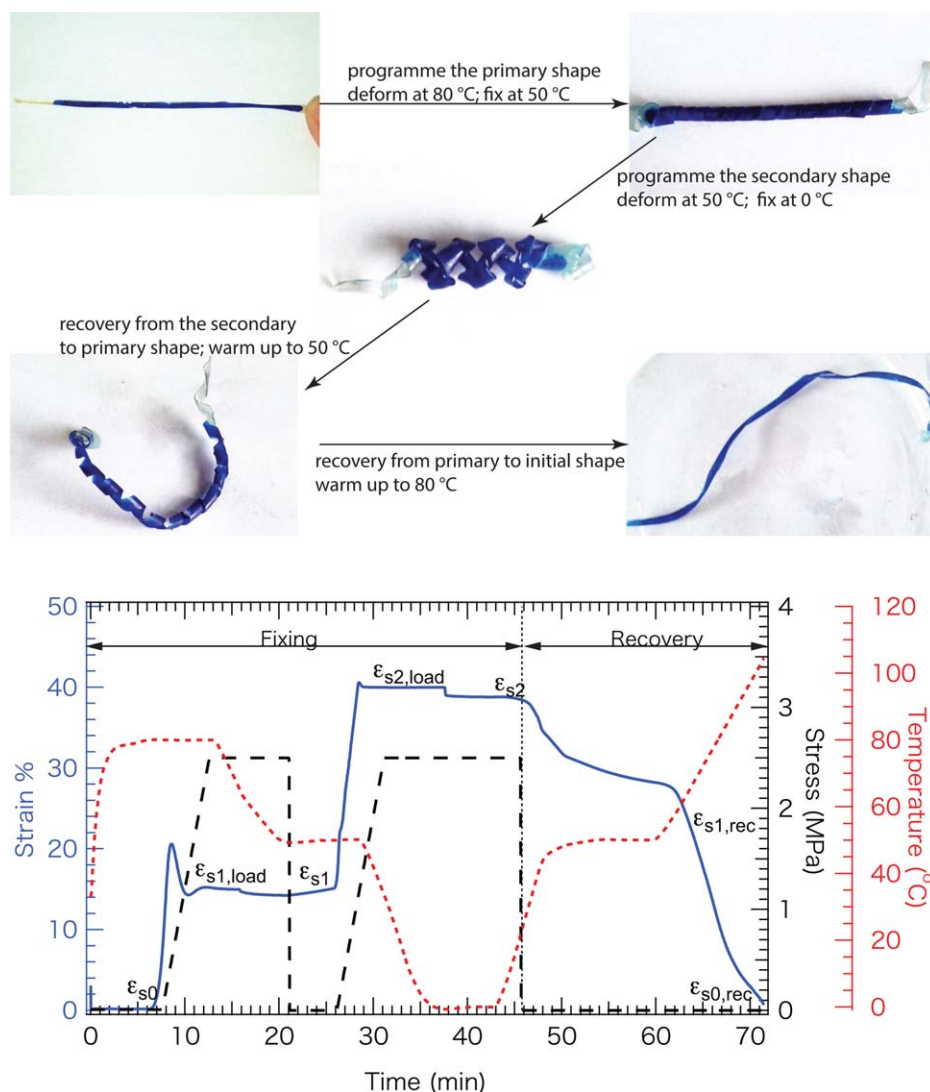


**Figure 6.** Visual demonstration of secondary shape programmed by using triple SME (top). The results of cyclic thermomechanical investigation for triple SME (bottom).  $R_f(s0-s1)$  and  $R_f(s1-s2)$  are 94% and 97%, respectively.  $R_r(s1-s0)$  and  $R_r(s2-s1)$  are 98% and 96%, respectively. [Color figure can be viewed in the online issue, which is available at [wileyonlinelibrary.com](http://wileyonlinelibrary.com).]

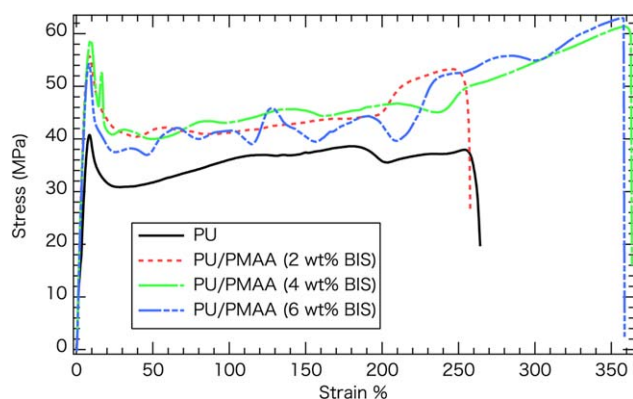


**Figure 7.** The stress-strain curves of PU/PMAA (3:1) with different crosslinker concentrations. [Color figure can be viewed in the online issue, which is available at [wileyonlinelibrary.com](http://wileyonlinelibrary.com).]

Michael addition.<sup>11,21</sup>In the later one, the polymer composite was macroscopically homogeneous, which largely increased the mechanical properties as well as triple SME. Since the shape recovery is driven by conformational entropy, the SME is highly reliant on the construction of composition. With the combination of our results, a strong correlation between microstructure

**Table II.** Ultimate Stresses and Maximum Strains Obtained from Figure 7

Samples	BIS (wt %)	Ultimate stress (MPa)	Extensional strain (%)
PU	0	40.76	259.71
PU/PMAA	2	55.74	255.20
	4	61.37	362.47
	6	62.96	357.09

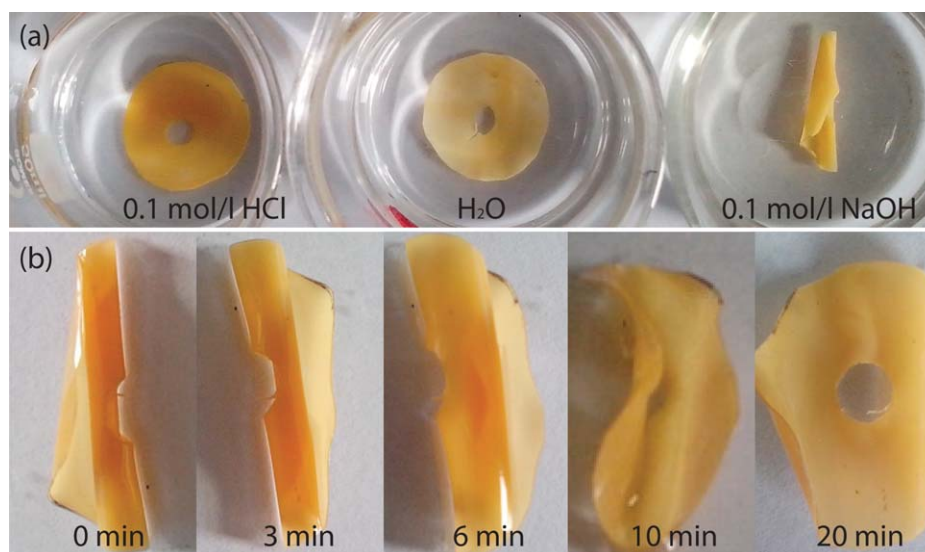


**Figure 8.** Shape change induced by (a) pH and (b) water. The shape of the specimen curled in a 0.1 mol/L NaOH solution, and when the specimen put in water or acidic solutions, the original shape is recovered. [Color figure can be viewed in the online issue, which is available at [wileyonlinelibrary.com](http://wileyonlinelibrary.com).]

and triple-SME was found. In the study, these two reversible phase transitions were provided by the soft segment of PU at its  $T_m$  and PMAA at its  $T_g$ . The results of DSC exhibited clearly that the  $T_g$  of PMAA is closely related to the weight ratio of PU/PMAA. With decreasing the content of PMAA,  $T_g$  shifted to lower temperature, and diminished at PU/PMAA = 5:1. Although the DSC curves of the specimen with PU/PMAA = 2:1 exhibit better phase separation, we did not observe triple SME. The similar results were found for the specimens with PU/PMAA = 4:1 and 5:1. These results may suggest two reversible phase transitions is in fact not the sufficient requirement to attain triple SME. For the specimen with PU/PMAA = 3:1, we observed the similar micro-structure as it is in Ref. 21. Even though the two reversible phase transition was not as pronounced as it is for PU/PMAA = 2:1, the specimen with PU/PMAA = 3:1 exhibited better triple-SME.

#### Water and pH-Induced SME

For pH-induced SME, there is a volume change corresponding to pH change. The mechanism is similar to temperature-induced SME. In general, there are two phases in temperature-induced

SMPs on molecular scale, which are switching phase and fixing phase. Switching phase is reversible phase with low switch transition temperature and fixes the temporary shape by forming physical cross-links; fixing phase is irreversible phase and determines the permanent shape.<sup>31</sup> In this study, PU/PMAA composite is composed of these two phases on molecular level. The fixing phase is the hard segment of PU, which determines the permanent shape and is stable at all pH; the switching phase (reversible phase) is the cross-linked PMAA mainly with also the soft segment of PU, which respond to pH change. The carboxylic groups in PMAA as pH-responsive units are sensitive to pH-change in solution. The carboxylic group in high pH solutions is ionized. Because of the electrostatic interaction between charged carboxylic groups, the soft segments in PU start sliding, which results a shape change in alkaline solution. On the other hand, when pH of solution is acidic, the carboxylic groups are protonated, where the reduced electrostatic force leads to a recovery to its initial shape.

With regard to water-induced SME, it is for the most part because of the cross-linked PMAA. Water molecules penetrate the PMAA network. This leads to the decrease of storage modulus because of the plasticizing effect of solution molecules on cross-linked PMAA.<sup>32</sup> In general, the faster the decrease of storage modulus is, the faster the shape recovery will be. Since this percolation network formed by PMAA allows water molecules to penetrate, as a physical barrier throughout the PU matrix it prevents the stretched macromolecular chains from entropic recovery back to its original entanglement.<sup>33</sup> In addition, based on the results of the contact angle experiment, the composites become more hydrophilic with the increase of molar ratio of PMAA, as also shown in the swelling experiments. With increasing the molar ratio of PMAA in the composite, more water molecules are able to penetrate the polymer network, which may reduce the transition temperature.<sup>34</sup> When the transition temperature of the soft segment reaches room temperature, the soft segments start moving, which cause the shape change. Moreover, because of hydrogen bonding, such as: -COOH dimer, -COOH with C=O (in urethane and PBAG), NH and C=O (in urethane, PBAG and -COOH), it will

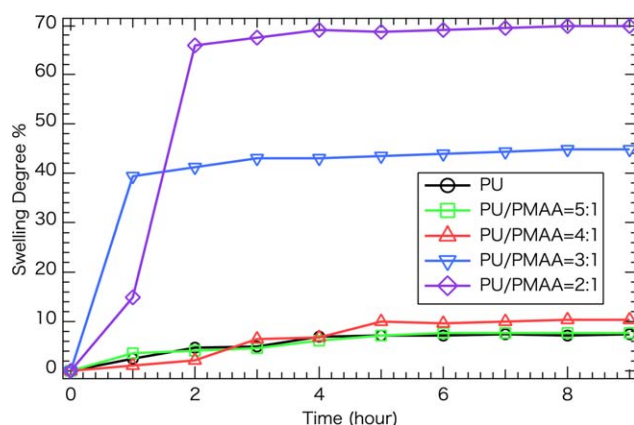


**Figure 9.** Swelling of PU/PMAA specimens in water. [Color figure can be viewed in the online issue, which is available at [wileyonlinelibrary.com](http://wileyonlinelibrary.com).]



reduce the mobility of the macromolecular chains; thus the PU/PMAA composite exhibits an excellent water-induced SME. So far, the mechanism for water-induced SME is under discovery, and on molecular level we have limited knowledge on relating the SME to the quantitatively bound water molecules on soft segments.

## CONCLUSIONS

Multi-stimuli SMPs were synthesized by using a strong segregative pair of polymers, PU and PMAA. The composite with PU/PMAA of 3:1 exhibited excellent thermo-induced triple-SME. By using the triple-SME, we demonstrated the possibility of forming secondary shape for SMPs, which, we expect, will benefit SMP applications. The SEM image of the polymer composite shows a polymer continuum with particles dispersed in it. In the discussion, we argued that the microstructures of the composites are essential to attain triple-SME. We may control the ratio of two components to obtain the desired microstructure. Apart from the thermo-induced triple-SME, the material exhibited shape change in respond to water and pH change, which we attributed to the addition of PMAA in the composite.

## ACKNOWLEDGMENTS

W.W. thanks QianRen Project for financial support. R.L.W. acknowledges National Natural Science Foundation of China (grant number 51063007).

## REFERENCES

1. Xie, T. *Polymer* **2011**, *52*, 4985.
2. Zhao, Q.; Jerry Qi, H.; Xie, T. *Prog. Polym. Sci.* **2015**.
3. He, Z.; Satarkar, N.; Xie, T.; Cheng, Y. -T.; Zach Hilt, J. *Adv. Mater.* **2011**, *23*, 3192.
4. Mather, P. T.; Luo, X.; Rousseau, I. A. *Annu. Rev. Mater. Res.* **2009**, *39*, 445.
5. Lendlein, A.; Kelch, S. *Angew. Chem. Int. Ed.* **2002**, *41*, 2034.
6. Yen, H.-J.; Liou, G.-S. *Polym. J.* **2015**, *10*.
7. Liu, C.; Qin, H.; Mather, P. T. *J. Mater. Chem.* **2007**, *17*, 1543.
8. Xie, T. *Nature* **2010**, *464*, 267.
9. Huang, W. M.; Yang, B.; Zhao, Y.; Ding, Z. *J. Mater. Chem.* **2010**, *20*, 3367.
10. Inoue, K.; Yamashiro, M. *Polym. J.* **2009**, *41*, 586.
11. Xie, T.; Xiao, X.; Cheng, Y.-T. *Macromol. Rapid Commun.* **2009**, *30*, 1823.
12. Goethals, E. J.; Reyntjens, W.; Lievens, S. *Macromol. Symp.* **1998**, *132*, 57.
13. Liu, G.; Ding, X.; Cao, Y.; Zheng, Z.; Peng, Y. *Macromol. Rapid Commun.* **2005**, *26*, 649.
14. Bai, Y.; Zhang, X.; Wang, Q.; Wang, T. *J. Mater. Chem. A* **2014**, *2*, 4771.
15. Bellin, I.; Kelch, S.; Lendlein, A. *J. Mater. Chem.* **2007**, *17*, 2885.
16. Yu, K.; Xie, T.; Leng, J.; Ding, Y.; Jerry Qi, H. *Soft Matter* **2012**, *8*, 5687.
17. Ge, Q.; Luo, X.; Iversen, C. B.; Mather, P. T.; Dunn, M. L.; Qi, H. *J. Soft Matter* **2013**, *9*, 2212.
18. Wang, W.; Arne Sande, S. *Eur. Polym. J.* **2014**, *58*, 52.
19. De Gennes, P.-G. *Scaling Concepts in Polymer Physics*; Cornell University Press, **1979**.
20. Leng, J.; Lan, X.; Liu, Y.; Du, S. *Prog. Mater. Sci.* **2011**, *56*, 1077.
21. Chatani, S.; Wang, C.; Podgórski, M.; Bowman, C. N. *Macromolecules* **2014**, *47*, 4949.
22. Yamashiro, M.; Inoue, K.; Iji, M. *Polym. J.* **2008**, *40*, 657.
23. Tanaka, H.; Suzuki, T.; Hayashi, T.; Nishi, T. *Macromolecules* **1992**, *25*, 4453.
24. Wang, W.; Arne Sande, S. *Polym. J.* **2015**, *47*, 302.
25. Glotzer, S. C.; Di Marzio, E. A.; Muthukumar, M. *Phys. Rev. Lett.* **1995**, *74*, 2034.
26. Williams, R. J. J.; Rozenberg, B. A.; Pascault, J.-P. *Reaction-Induced Phase Separation in Modified Thermosetting Polymers*; In *Polymer Analysis Polymer Physics*; Springer, **1997**; p 95.
27. Jinlian, H. *Advances in Shape Memory Polymers*; Elsevier, **2013**.
28. Tsavalas, J. G.; Sundberg, D. C. *Langmuir* **2010**, *26*, 6960. PMID: 20085370.
29. Wang, W.; Sande, S. A. *Langmuir* **2013**, *29*, 6697.
30. Kyu Kim, B.; Yup Lee, S.; Xu, M. *Polymer* **1996**, *37*, 5781.
31. Han, X.-J.; Dong, Z.-Q.; Fan, M.-M.; Liu, Y.; Wang, Y.-F.; Yuan, Q.-J.; Li, B.-J.; Zhang, S. *Macromol. Rapid Commun.* **2012**, *33*, 1055.
32. Wu, T.; O'Kelly, K.; Chen, B. *J. Polym. Sci. B Polym. Phys.* **2013**, *51*, 1513.
33. Dagnon, K. L.; Shanmuganathan, K.; Weder, C.; Rowan, S. J. *Macromolecules* **2012**, *45*, 4707.
34. Yang, B.; Huang, W. M.; Li, C.; Li, L. *Polymer* **2006**, *47*, 1348.